Eighth Australasian Fluid Mechanics
Conference, University of Newcastle,
N.S.W., 28 November/2 December 1983.

QUALITATIVE INVESTIGATION ON GOERTLER VORTICES

S.H. WINOTO

DEPARTMENT OF MECHANICAL AND PRODUCTION ENGINEERING

NATIONAL UNIVERSITY OF SINGAPORE, KENT RIDGE, SINGAPORE - 0511

SUMMARY Naturally developing longitudinal vortices in the concave surface laminar boundary layer of a water channel with 180° bend have been visualized by using hydrogen bubble technique. Different views, especially the transverse cross-sectional views of the vortex flow pattern at Reynolds number (based on bulk velocity and channel width) of 2700 are presented. At bend angle of around 90°, when Goertler number reached 10.8, spanwise wandering of the vortices, as also reported previously, was observed.

1. NOTATION

a	channel width
b	depth of water
G_Θ	Goertler number $Re_\Theta (\Theta/r)^{1/2}$
P	vortex wavelength parameter $(u_b r/\nu)(\lambda/r)^{3/2}$
Re_a	Reynolds number $u_b a/\nu$
Re_Θ	momentum thickness Reynolds number $u_b \Theta/\nu$
r	radius of concave wall
u,v,w	velocity components in x,y,z, directions respectively
u_b	bulk velocity (volume flow rate/ab)
x,y,z	co-ordinates in streamwise, pitchwise (normal), spanwise directions respectively
β	vortex amplification
δ	boundary layer physical thickness
Θ	boundary layer momentum thickness
λ	vortex wavelength
ν	kinematic viscosity
Φ	angular co-ordinate measured from bend entry

Subscripts

cr	critical value
tr	transition value
pw	potential wall value

2. INTRODUCTION

The longitudinal counter - rotating vortices that may develop in the boundary layer along a concave surface (which are known as Goertler vortices as sketched in Fig.1) are due to dynamic instability that would arise when the centrifugal force becomes so large that the radial pressure gradient and viscous forces can no longer damp out small disturbances. Since concave surfaces exist in many fluid dynamic applications, such as those in turbomachinery, the existence of such longitudinal vortices can not be ignored if calculations of boundary layer development and heat transfer are to be reliable. The aim of the present work is to provide qualitative information of the velocity field within naturally occuring Goertler vortices on concave surfaces (that is, the vortex wavelength is not pre-defined by an artificial disturbance) which might be required, for example, in a study of heat transfer, as well as inertial deposition of solid particles (in the case of gas turbines) or droplets (in the case of steam turbines) from two phase flows on turbine blade pressure (concave) surfaces.

No existing theory will predict the vortex wavelength λ. However, Smith's (1955) stability chart, showing lines of constant β on a plot of Goertler number G_Θ ($=Re_\Theta (\Theta/r)^{1/2}$, the convectional stability parameter) versus $2\pi\Theta/\lambda$ (wave number times momentum thickness), provides a means of estimating the most likely wavelength in the absence of any strong peaks in the initial spectrum of disturbance wavelengths. Smith himself suggested that the wavelength having the greatest cumulative amplification, $\int\beta.dx$ is the best estimate. In practice, some physical non-uniformity in the flow boundaries (e.g., the edge of a settling chamber screen in a laboratory rig, or spanwise roughness variation on a turbine blade) is likely to determine the wavelength, which will not necessarily be uniform across the span.

By forcing a wavelength different from that occuring naturally, Tani and Aihara (1969) found that amplification of the vortices was only weakly selective to wavelength, as might be expected from the flatness of the neutral stability curve ($\beta=0$) in the region of the critical Goertler number (minimum G_Θ for instability).

Another aspect of concave surface flows requiring further investigation in transition in the presence of Goertler vortices. The small amount of data presently available suggests that it may be possible to relate the start of transition to a value of G_Θ which is a function of turbulence level and Θ/r (where r is the surface radius of curvature). Values of G_Θ between 6 and 9 have been reported by Liepmann (1945) at the beginning of transition depending on the free-stream turbulence level. A different transition criterion was proposed by Smith (1955), based on $\int\beta.dx$ reaching a value of around 9; this was supported by Kemp's (1977) cascade measurements.

In the present work, the vortices were formed in the concave surface laminar boundary layer of a water channel with 180° bend, which was part of a closed circuit water flow. Standard hydrogen bubble technique was used to visualize the vortex flow pattern at different views. The transverse cross-sectional views of Goertler vortices (which have not

been reported, and can provide qualitative information on the pitchwise velocity component, strongly responsible for heat transfer and inertial deposition effects) are obtained.

3. EXPERIMENTAL DETAILS

The closed-circuit water flow was similar to that described by Winoto and Crane (1980), and consisted of an electric motored pump, "Rotameter" flow meter, heat exchanger and an open-surface test channel (chosen to facilitate flow visualization) as shown in Fig. 2. The heat exchanger, water-cooled, was used to maintain the water temperature constant during the experimental runs. Water was pumped through multiple hoses into a settling chamber which contained four gauze screens. A 5:1 area ratio, two-dimensional contraction preceded a straight section of length 2.0 a, where a is the channel width equal to 40 mm, followed by the 180° bend test section whose outerwall had a radius r = 10.5 a. The test section geometry is defined in Fig. 3. The gauze screens and contraction provided a reasonably uniform entry flow into the test section at low free-stream fluctuation intensity. Downstream of the bend, a 7.0 a straight section was followed by a diffuser and an exit chamber of similar dimensions to the settling chamber. The vertical walls were formed from heated sheet materials and special attention was paid to smoothing the joints between wall sections upstream of the concave wall; all surfaces were hydraulically smooth. However, precautions such as siting the rig in an isolated, constant temperature room, as described by Wortmann (1964 and 1969) were not taken in the present work.

Flow visualization was made by using the standard hydrogen bubble technique with a 50 μm diameter stainless steel wire as the hydrogen bubble producing cathode. This visualization techniques such as dye injection and flash photolysis (photochromic) methods as described by Winoto and Crane (1980).

The aspect ratio b/a, determined by the choice of the depth b of water, was 6.0, a compromise which minimized the pump capacity while ensuring a sufficiently uniform inlet flow and avoiding unacceptable secondary flow effects. Visualization showed that the longitudinal vortex system was not noticeably affected by the end-wall secondary flow or surface effects in at least the middle 80 per cent of the span.

The visualizations presented here were obtained only at Reynolds number Re_a of 2700 (which gave the best visualization results) and the corresponding bend entry Dean number $Re_a\,[a/(r - \frac{1}{2}a)]^{\frac{1}{2}}$ of 860.

Data recordings were made by using a still SLR camera whose viewing direction was always set perpendicular to the lighting beam direction.

4. RESULTS AND DISCUSSION

Plates 1 (a) and (b) respectively show the side view, and top view (or "vortex roll") of Goertler vortex flow pattern, while Plates 2 (a), (b), (c), (d) and (e) show the transverse views only at bend position Φ of 73° with the hydrogen bubble wire (which was placed upstream of Φ = 73°) at different pitchwise (normal) positions y of 1mm, 10mm, 15mm, 20mm and 25mm respectively. The mean vortex wavelength was found to be 22.7mm. Using "constant wavelength curve method" as described by Winoto (1980) on Smith's stability chart, the wavelength of the most probable vortices to occur (i.e. the vortices which receive maximum local amplification) is predicted to be 19mm (in the case of the constant wavelength parameter P = 272). Using "vortex growth diagram method" as described by Smith (1955), the predicted vortex wavelength was found to be 22.0mm. However, since longitudinal velocity profiles u(y), were not obtained, the Goertler number G_Θ at a bend position was estimated based on Blasius boundary layer assumption as also done by Smith (1955) for example: at the bend position Φ = 73°, G_Θ = 9.37.

Visualizations at some bend positions upstream of Φ = 73°, produced similar but less pronounced patterns than those shown in Plates 1 and 2 (i.e. with the same constant wavelength for every vortex pair). However, at Φ = 90° (G_Θ = 10.77) low frequency (of about 0.5 Hz) vortex wandering in the spanwise direction, over a distance less than λ, was observed which made estimation of vortex wavelength not possible. This vortex wandering phenomenon was also reported previously by Wortmann (1969), Aihara (1979), and Winoto and Crane (1980).

According to Wortmann (1969), this vortex oscillation is a higher mode (of third order) of Goertler vortex instability. (The second order mode being characterised by deformed but non-oscillating vortex pattern). Since the phenomenon of transition is in principle unsteady, this vortex unsteadiness might be associated with the start of the concave surface boundary layer transition which was triggered at the spanwise positions where the boundary layer was thickest. Streamwise velocity measurements using a laser anemometer carried out by Winoto and Crane (1980) (for the case of r/a = 3.5 at Re_a = 3800) revealed high fluctuation intensities at these thick boundary layer positions. However, according to "$G_{\Theta tr}$ = 9 transition criterion "as suggested by Liepmann (1945) for low turbulence intensity of 0.06%, the transition should start at Φ = 69°, while according to "$\int_{x_{cr}}^{x_{tr}} \beta\, dx = 9$ transition criterion" proposed by Smith (1955), Φ_{tr} should be 65°.

Experiments at some lower Reynolds numbers showed pronounced buoyancy effect on hydrogen bubbles since a larger (than normally recommended) hydrogen bubble wire of 50 μm was used, while at higher Reynolds numbers, turbulent diffusion effect on the bubbles was quite significant.

Fig. 4 shows the positions of the present conditions at bend positions Φ of 30°, 45° and 73°, and those obtained by Winoto and Crane (1980) to be well inside the unstable region in the Smith's stability diagram. However, Winoto and Crane (1980) used potential wall velocity u_{pw} (obtained by extrapolation of the u(y) profiles in the coreflow) to define the relevant parameters in Fig. 4, whereas in the present work, bulk velocity u_b (volume flow rate/ab) is used instead, since u(y) profiles were not obtained.

5. CONCLUSIONS

1. Goertler vortex flow patterns have been visualized in a 180° bend water channel by means of hydrogen bubbles. Unlike previously reported visualizations, transverse cross-sectional views were obtained which confirm the wavy variations in boundary layer physical thickness along the spanwise direction due to the presence of such vortices.

2. The mean vortex wavelength (for $\phi < 90°$ as found to be very close to the predicted wavelengths obtained by using "constant wavelength curve" and "vortex growth diagram" methods. Variation of vortex wavelength with spanwise position is at present attributed to unidentified physical features of the channel.

3. Vortex wandering in the present work (at Re_a = 2700 and r/a = 10.5) occurred at $\phi \approx 90°$ when G_Θ reached 10.8, whereas in the work reported by Winoto and Crane (1980), at Re_a = 3800 and r/a = 3.5 this unsteadiness occurred at $\phi \approx 76°$ when G_Θ reached about 12. Both concave surface boundary layer transition prediction methods, namely, the "$G_{\Theta tr}$=9" and "$\int_{x_{cr}}^{x_{tr}} \beta dx = 9$" criteria, predicted the starts of transition at ϕ =69° and ϕ =65° respectively.

6. REFERENCES

AIHARA, Y. (1979) Goertler vortices in the nonlinear region, in Recent Developments in Theoretical and Experimental Fluid Mechanics, Eds. W. Muller, K.G. Roesner and B. Schmidt, Springer-Verlag, pp. 331-338.

KEMP, A.S. (1977) The boundary layer on the pressure force of turbine blades in cascade, Ph.D. Thesis, Cambridge University.

LIEPMANN, H.W. (1945) Investigation of boundary layer transition on concave walls, NACA Adv. Conf. Rep. 4J28.

SMITH, A.M. (1955) On the growth of Taylor-Goertler vortices along highly concave walls, Quart. Appl. Math., 13 pp. 233-262.

TANI, I. and AIHARA, Y. (1969) Goertler vortices and boundary layer transition, Zeit. Angeur. Math. Phys., 20, pp. 609-618.

WINOTO, S.H. (1980) Longitudinal vortices in concave surface boundary layers, Ph.D. Thesis, London University.

WINOTO, S.H. and CRANE, R.I. (1980) Vortex structure in laminar boundary layers on a concave wall, Int. J. Heat & Mass Fluid Flow, 2, pp. 221-231.

WORTMANN, F.X. (1964) Experimentelle Untersuchungen laminarer Grenzschichten bei instabiler Schichtung, Proc. 11th Int. Congr. Appl. Mech., Munich, pp. 815-825.

WORTMANN, F.X. (1969) Visualization of transition, J. Fluid Mech., 38, pp. 473-480.

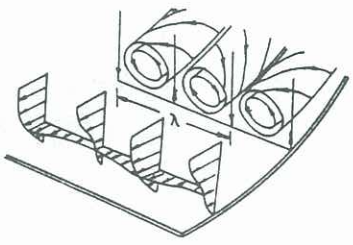

FIG. 1 SKETCH OF GOERTLER VORTICES

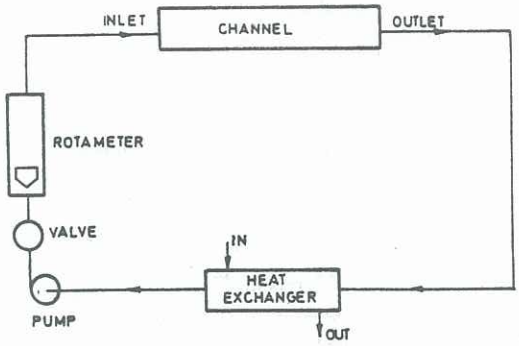

FIG. 2. BLOCK DIAGRAM OF FLOW CIRCUIT

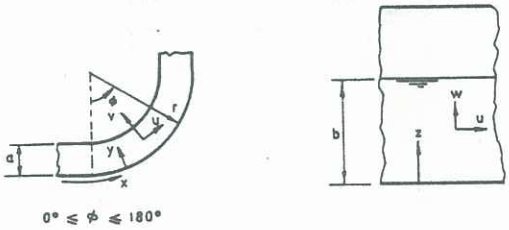

a) TOP VIEW b) SIDE VIEW

FIG. 3. TEST SECTION GEOMETRY WITH CO-ORDINATE AND VELOCITY COMPONENT DEFINITIONS

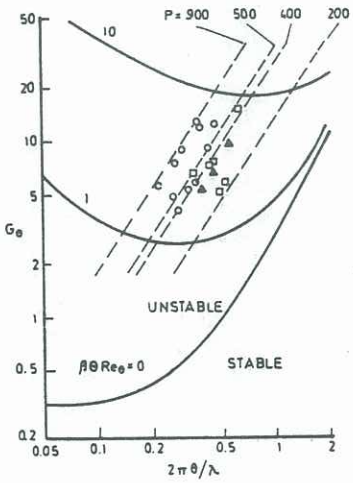

FIG 4. GOERTLER VORTEX STABILITY DIAGRAM

PRESENT DATA : ▲ r/a = 10.50
DATA FROM [12]: ○ r/a = 3.50
□ r/a = 2.75

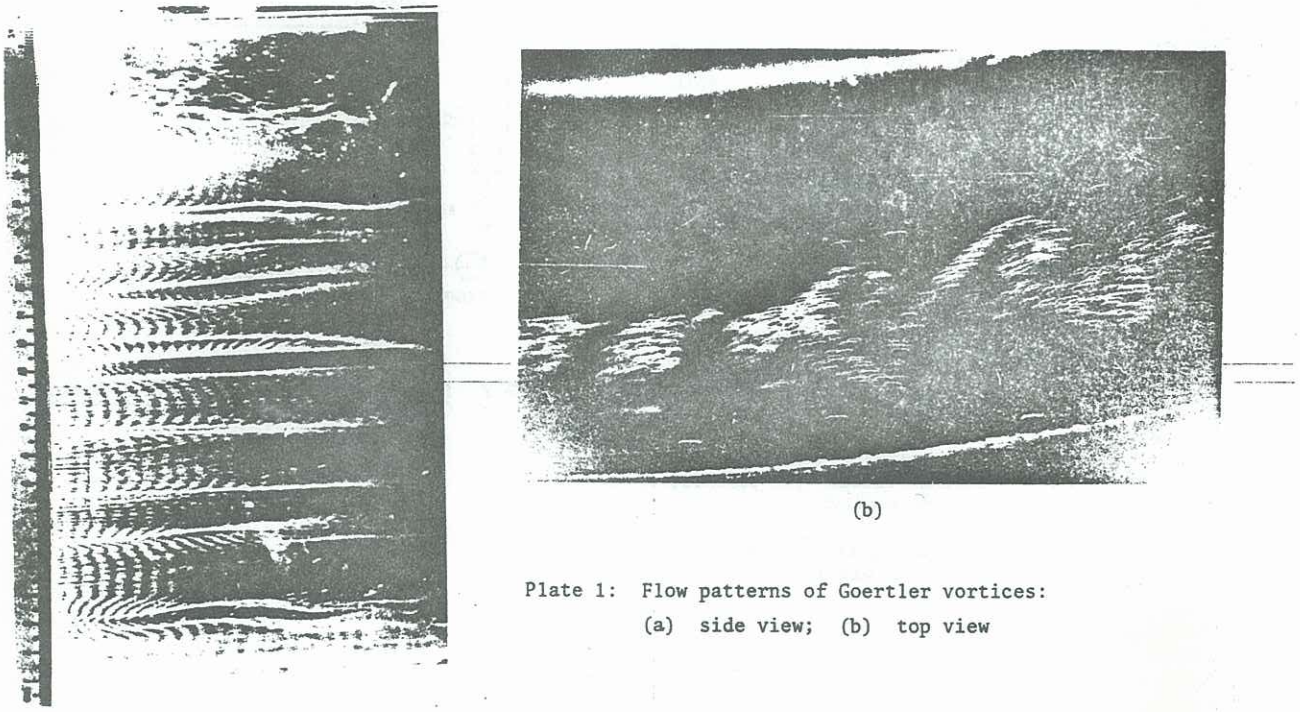

(a) (b)

Plate 1: Flow patterns of Goertler vortices:
(a) side view; (b) top view

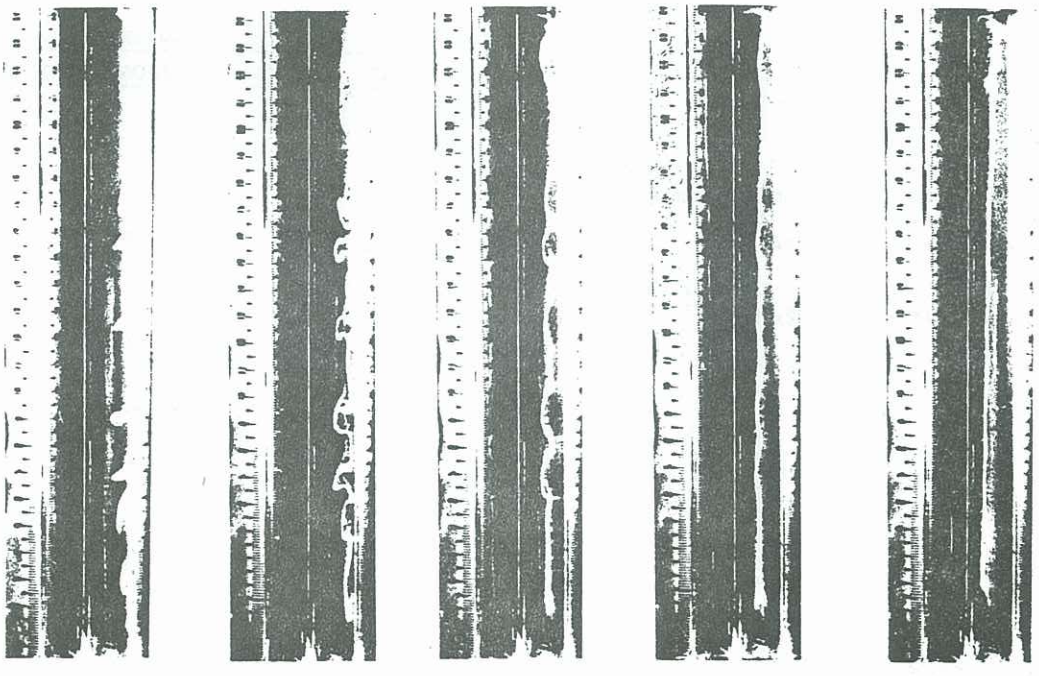

(a) (b) (c) (d) (e)

Plate 2: Transverse cross-sectional views of Goertler vortices at ϕ = 73° (Re_a = 2700) for different hydrogen bubble wire positions: (a) y = 1mm; (b) y = 10mm; (c) y = 15mm; (d) y = 20mm and (e) y = 25mm.